STUDIES ON ATRAZINE PESTICIDE REMOVAL USING SYNTHESIZED MGO/ACTIVATED CARBON NANOCOMPOSITE

Variganji Gowthami[1], Bandela Sowjanya[2], Malluvalasa Nagendra Kumar[3], Meena Vangalapati[4*]

Abstract

Magnesium oxide nanoparticles (MgONP) have been synthesized and used to make a MgO/activated carbon nanocomposite which was used to remove atrazine (ATZ) from aqueous solutions. Fourier transform infrared (FTIR) spectroscopy, elemental analysis, and SEM were used to examine the synthesised MgO/activated carbon nanocomposite. The adsorption process was examined in batch mode employing a number of variables, including temperature, pH, ATZ concentration, agitation time, and adsorbent dosage. The conditions of 35 minutes of agitation, 0.1 g/L of adsorbent dose, pH 8, 323 K of temperature, and 10 mg/L of ATZ concentration were shown to be the most efficient adsorption method for removing ATZ. The experimental findings show that the highest adsorption capacity is 625.5 mg g^{-1}, which is nearly equal to the estimated qe of 666.6 mg g^{-1}

Keywords: Nanocomposite; Atrazine; Magnesium Oxide; Activated Carbon;

[1,2] Research Scholar, Chemical Engineering Department, AUCE, Visakhapatnam, A.P, 530003, India
[3] Manager, Process Department, Indian Farmers Fertilizers, Kalol, Gujarat, 302721, India
[4*] Professor, Chemical Engineering Department, AUCE, Visakhapatnam, A.P, 530003, India

***Corresponding Author:** Meena Vangalapati
*Professor, Chemical Engineering Department, AUCE, Visakhapatnam, A.P, 530003, India

DOI: 10.48047/ecb/2023.12.si10.00330

1. Introduction

To satisfy agricultural production objectives, herbicide and pesticide use is increasing year after year. They are the main cause of pollution in the environment, which has a direct impact on water quality and finally affects humans [1]. It is employed as a pre- and post-emergent herbicide to manage grasses and broadleaf weeds in crops like sorghum, sugarcane, and maize. ATZ is often found in surface and ground rivers due to its high soil mobility. ATZ has been found to harm aquatic species and interfere with the generation of healthy human hormones in numerous studies. Because ATZ is regularly discovered in drinking water, the USEPA has set a contamination limit of 3 parts per billion (ppb) [2].

These statistics from the wastewater have been the foundation for many ATZ eradication methods. ATZ cannot be removed using conventional techniques including filtering, coagulation, chemicals, or biological treatments. As a result, having a well-organized management structure is crucial. Adsorption techniques must be simple, easy to use, and very successful at removing impurities from water [3].

With the use of nanomaterials, nanoparticles, or nano adsorbents for the removal of various contaminants from water, wastewater, and polluted air streams, nanotechnology has recently arisen as a fresh and fascinating research area. For the past ten years, environmental contaminants have been treated and remedied using nanocrystalline metal oxides as a potential adsorbent [4, 5].

A common metal oxide termed MgO nanoparticles can be easily produced from affordable raw resources such sodium salts, magnesium salts, and magnesium-containing rocks like dolomite and magnesite. In addition to their antibacterial effects, MgO nanoparticles also exhibit better biocompatibility, non-toxicity, a high surface area to volume ratio, UV blocking properties, and photocatalytic activity, to list a few. As a result, nanometer-sized MgO-based bactericides, ceramic materials, catalysts, hazardous waste remediation materials, insulators, and refractory materials have gained prominence significantly [6]. Since it has long been known that activated carbon (AC) can adsorb a variety of organic compounds, including colours and coloured contaminants, odorous chemicals, and pesticides, it stands out among the many adsorbents studied for the removal of ATZ [7]. A novel strategy to improve adsorbent activity performance is the combination of these two adsorbent materials [8]. Several research have been successfully conducted using the incorporation of magnesium oxide nanoparticles with AC in the production of adsorbents for water treatment.

By utilising a compound made of graphene oxide and iron oxide nanoparticles, M. B. Andrade et al. [8] conducted novel study on the removal of ATZ from water samples. A 42.5 mg/g adsorption capability was found to exist. Heena Khawaja et al. [3] employed a nano-composite made of carboxymethyl cellulose and magnetic graphene oxide to extract ATZ from water (GO-CMC-Fe). A detailed kinetic and thermodynamic investigation was conducted. The largest quantity of adsorption obtained, they continued, was 194 mg/g. Elhassan A. Allam et alproduction.'s of NiO, ZnO, and NFe3O4 nanoparticles [9] resulted in N-NiO@N-Fe3O4@N-ZnO, which had an adsorption capacity of 100.0 mg/g for the elimination of ATZ. MgONP-AC was created by V.R. Myneni et al. [10] to remove the dye methylene blue and obtained 207 mg/g adsorption capacity. The current research focuses on the chemical precipitation of activated carbon/MgO nanocomposite. On the adsorption of ATZ, the effects of the most essential factors were investigated.

2. Materials and methods

2.1. Synthesis procedure of Magnesium Oxide Nanoparticles

The magnesium oxide nanoparticles were made utilising the chemical precipitation method and were made with PVP, ammonium hydroxide, and magnesium nitrate hexahydrate. 30 minutes of stirring on a magnetic stirrer were spent stirring a 0.5M Mg (NO3)2 6H2O solution with 2g of PVP added. A 0.5M ammonium hydroxide solution was gradually added as the mixture reached a pH of 10.5 in the process. The final solution was left at room temperature for 24 hours in order to precipitate magnesium ions. After samples were centrifuged at 4000 rpm for 15 minutes to remove byproducts and impurities, the precipitate was filtered, repeatedly rinsed with demineralized water, and then treated with ethanol [10].

2.2. Synthesis process of MgO/Activated carbon Nanocomposite

By soaking 5 g of commercial activated carbon in 250 ml of ethanol and 1 g of MgO nanoparticles in 50 ml of ethanol for three hours, a MgO/Activated carbon nanocomposite was made. 12 hours were spent at room temperature with the mixture being stirred at 300 rpm. The resultant particles were centrifuged for 15 minutes and heated to 80°C. It was then washed with distilled water and allowed to air dry [10, 11]. MgO/activated carbon was the name given to the prepared composite (Fig. 1).

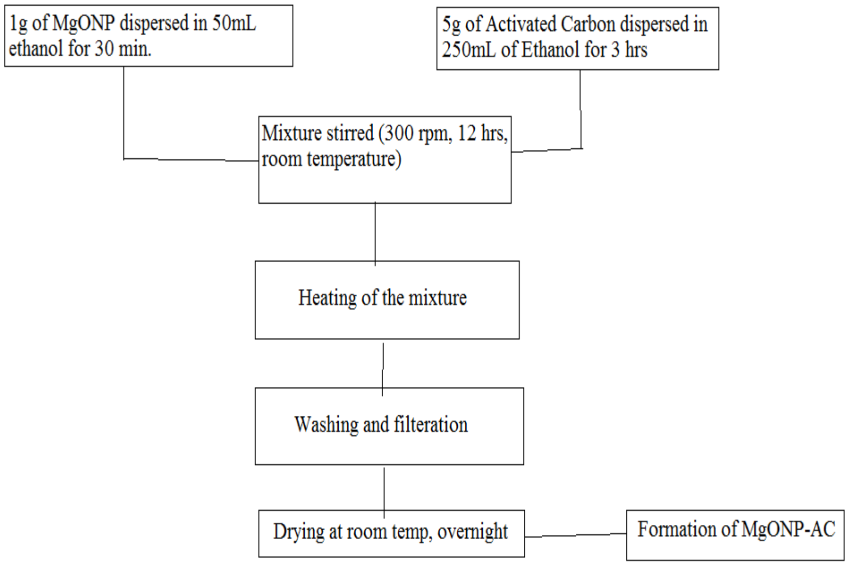

Figure. 1 Synthesis of MgO/activated carbon nanocomposite

2.3. Characterization

According to the SEM analyses (Fig. 2a), the MgO/activated carbon particle size is 2 m. Moreover, it has been noted that the MgO/activated carbon surface exhibits holes or cavities that can effectively absorb atrazine. The elemental analysis results (Fig. 2b), in MgO/activated carbon the weight fraction of C, N were 40.43%, 40.57% respectively, with the attachment of 16.69% of O and 1.82% of Mg. The evidence of attachment of MgO nanoparticles on the surface of activated carbon was observed.

2.4. Estimation procedure for ATZ

A UV-visible spectrophotometer was used to estimate ATZ levels. The procedure involves adding pyridine and an estimated amount of ATZ to a water bath for 15 minutes at 70^0C, allowing the mixture to cool to room temperature, and then adding sodium hydroxide, 4 amino acetanilide, HCl, and sodium lauryl sulphate to produce a yellow-orange end product [8]. And the extracted product was passed through a C_{18} cartridge. The coloured product obtained from the cartridge was extracted once more with methanol and measured at 460 nm at reagent blank, which yielded minimal absorbance at this wavelength.

2.5. Removal of ATZ using MgO/activated carbon

Batch adsorption studies were used to remove ATZ utilising MgO/activated carbon as the adsorbent. ATZ concentrations ranging from 10 to 100 mg/L were used to dissolve 0.1g of MgO/activated carbon in 100 mL of the ATZ aqueous solution. The contents of were shaken for fixed time intervals ranging from 5 to 60 minutes in an orbital shaker at 308 K. A digital pH metre was used to measure the pH of the ATZ solution, which ranged from 4 to 10. The solids were then separated by centrifugation at 4000 rpm for 15 minutes. The percentage removal of ATZ was obtained using the Eq.1 [12, 13]:

$$\%\ \text{Removal of ATZ} = \frac{(C_0 - C_e)}{C_e} \times 100 \qquad (1)$$

Where C_o, C_e are the initial and final concentration of the dye solutions respectively

2.6. Kinetics, Isotherms & Thermodynamics of adsorption

The kinetics of ATZ adsorption on MgO/activated carbon were investigated using pseudo-first-order and pseudo-second-order models. The adsorption equilibrium was established using the Langmuir and Freundlich adsorption isotherm models.

Three thermodynamic parameters associated with adsorption are standard free energy change (G), standard enthalpy change (H), and standard entropy change (S). The free energy of the sorption process is given by Eqs. 7, 8 [12] after accounting for the distribution coefficient Kc of the sorption process.

$$\Delta G = -RT\ln K_c \qquad (3)$$

$$K_c = \frac{C_{ad,e}}{C_e} \qquad (4)$$

Where, ΔG is standard free energy change, ΔH is standard enthalpy change and ΔS is standard entropy change, R as Universal gas constant, T as temperature in Kelvin and distribution coefficient (Kc)

3. Results and Discussion

3.1. FTIR specctroscopy

Figs. 2c and 2d depict the FTIR spectra for MgO/activated carbon and MgO/activated carbon with ATZ loaded. As can be observed from the images, the interaction with ATZ caused some of the peaks that are shown in the MgO/activated carbon FTIR spectra to alter positions or disappear entirely. The functional groups of ATZ may be the cause of the few additional peaks seen in the MgO/activated carbon FTIR spectra after being loaded with ATZ. Evidently, the produced MgO/activated carbon successfully adsorbed the ATZ molecules in the aqueous solution based on FTIR Spectroscopy. The distinctive band at 3647 cm^{-1} in the FTIR spectra of MgO/activated carbon is attributable to O-H bending vibrations. Because of the Mg-O functional groups, the presence of Magnesium Oxide nanoparticles produces peaks below 1000 cm^{-1} [10]. A band of C-C vibrations can be found at 1380-1440 cm-1. After ATZ adsorption, a faint peak developed at 1012cm^{-1}, which corresponds to C-O stretching. C-H bond vibrations were associated with the stretching frequency in 2944-2698 cm^{-1}.

(a)

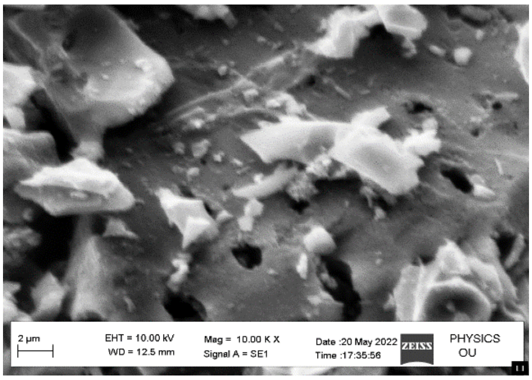

(b)

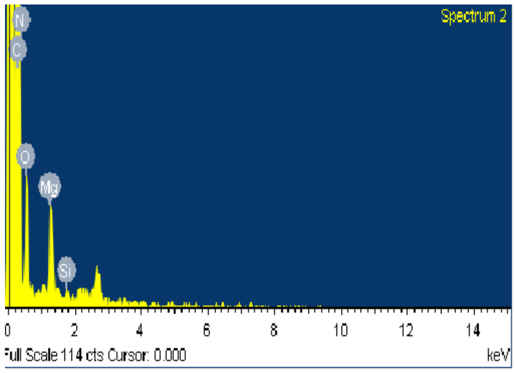

(c)

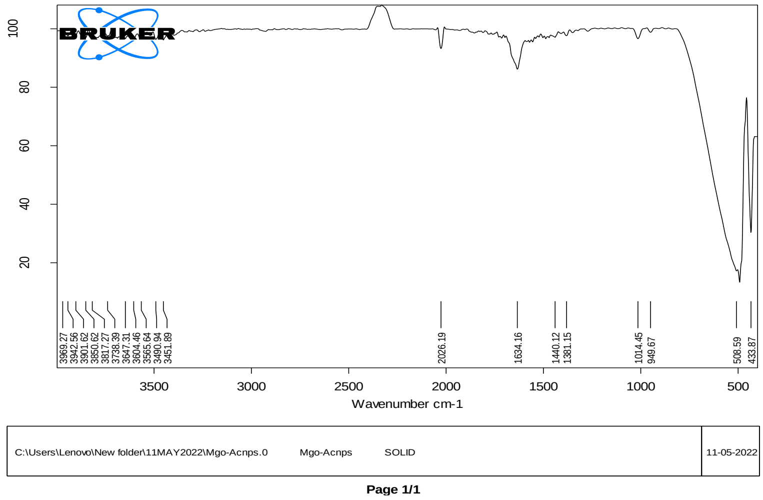

(d)

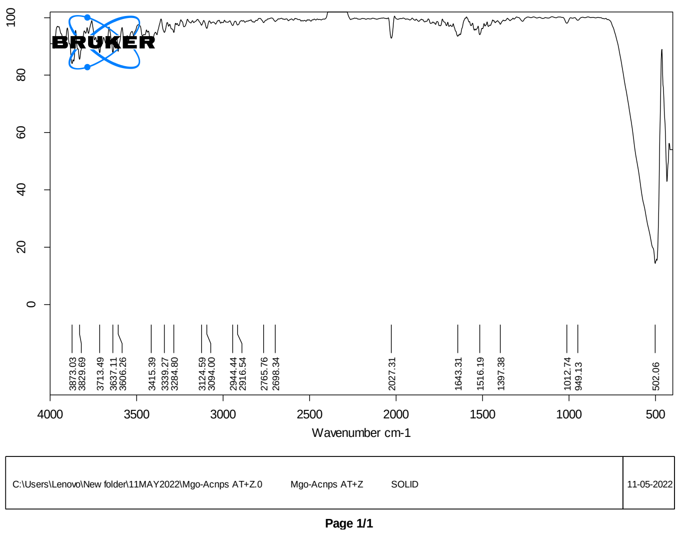

Figure.2 (a) SEM image (b) EDX analysis (c) FTIR for MgO/activated carbon (d) FTIR for ATZ loaded MgO/activated carbon

3.2. Effect of agitation time

The amount of ATZ eliminated raised as the agitation period increased from 5 to 35 minutes, as shown in fig. 3(a). Because maximum adsorption locations were more accessible during the initial exposure of the adsorbent, the removal rate was increased. The saturation of possible active sites on the adsorbent surface, which happened after 35 minutes, is what caused the removal rate to remain almost unchanged. As a result, the agitation duration for the removal of ATZ using MgO/activated carbon was determined to be 35 minutes, and it was used in further experiments.

3.3. Effect of adsorbent dosage

The impact of adsorbent dosage on ATZ adsorption on MgO/activated carbon was examined in the 0.02 to 0.12 g/L range. The MgO/activated carbon nanocomposite dosage in the ATZ solution (100 mg/L) was increased from 0.02 to 0.1 g/L to improve ATZ elimination (fig. 3(b)). Furthermore, the percent removal remains constant as the adsorbent dosage is increased. As a result, the best adsorbent dosage for ATZ adsorption was determined to be 0.1 g/L, and this dosage was used in the remaining batch experiments.

3.4. Effect of pH

The proportion of ATZ removed grew progressively as the pH raised from 4 to 8, then gradually declined at pH 9 and 10 (fig. 3(c)). The greatest removal of 83 percent was reported at pH 8. This could be owing to the deprotonation of the MgO/activated carbon nanocomposite, which strengthened the electrostatic interaction between the ATZ and the adsorbent [3].

3.5. Effect of concentrations of ATZ

The eradication percentage of ATZ decreased as the concentration of ATZ increased, as seen in fig. 3. (d). As a result, the quantity of active sites increases together with the concentration of ATZ solution. As a result, solutions with lower ATZ concentrations performed better at removal.

3.6. Effect of temperature

In order to see how temperature affected the outcomes while holding the other variables constant, the experiment was carried out at 308–323K. According to fig. 3, the removal efficiency grows as the temperature does (e). This result indicates that the adsorption of ATZ by MgO/activated carbon Nanocomposite is endothermic. The mobility and dispersion of ATZ molecules in solution increase with temperature.

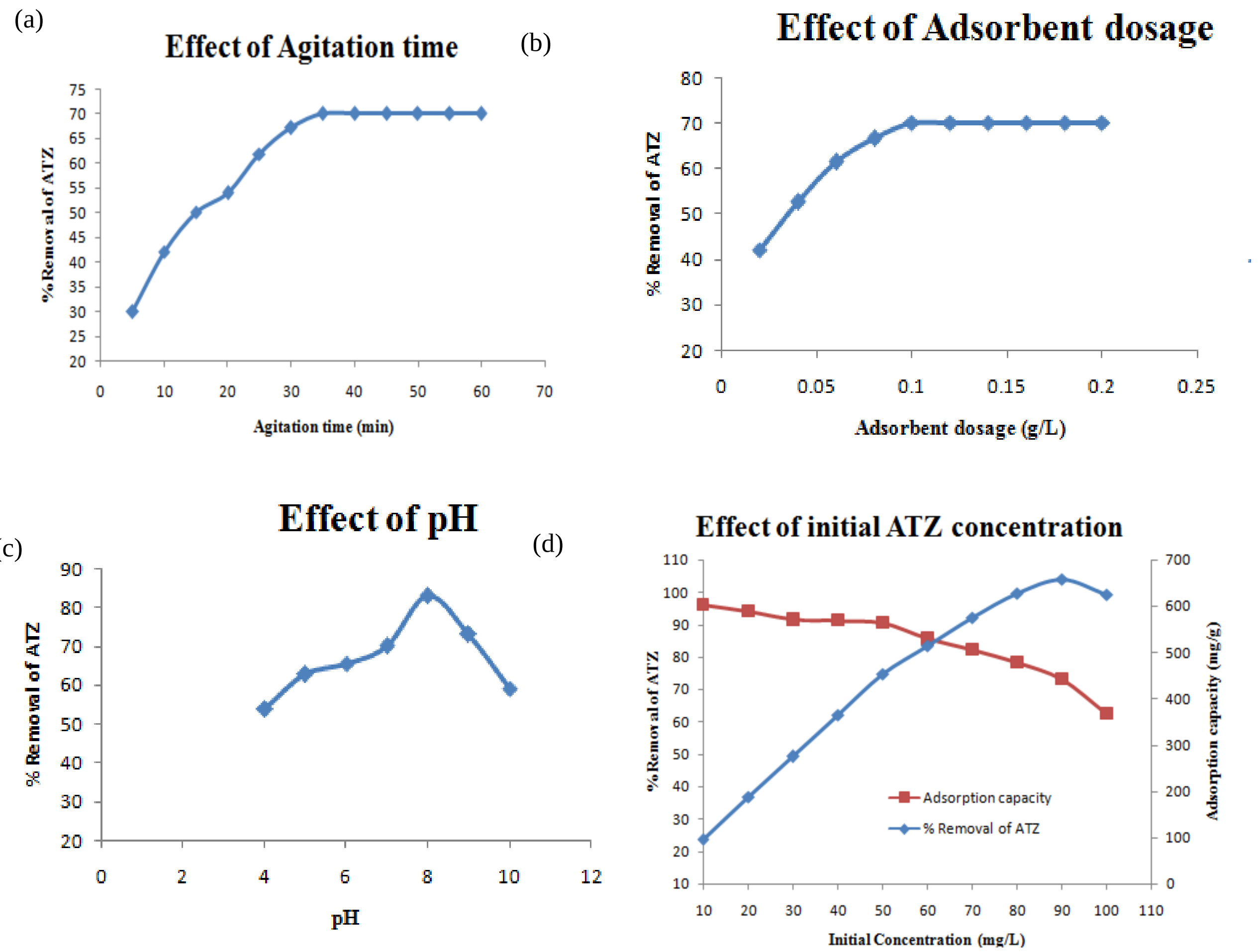

(e)

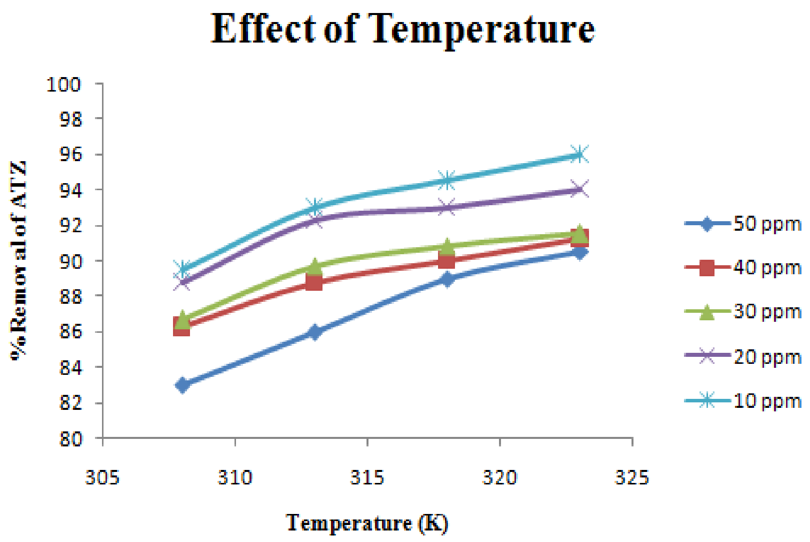

Fig.3. Effect of (a)Agitation time, (b) Adsorbent dosage, (c) pH, (d) Initial Concentrations of ATZ (e) Temperature

3.7. Adsorption kinetics, Isotherms & Thermodynamics

The fitted plots of several adsorption kinetic models are shown in Figures 4(a) and 4(b. The corresponding correlation coefficients evaluate each model's reliability (R2). The pseudo-second-order model best describes the process and rate of ATZ absorption by MgO/activated carbon Nanocomposite when the correlation coefficients of the pseudo-first-order (R^2 = 0.711) and pseudo-second-order (R^2 = 0.978) kinetic models are compared [14, 15].

Table 1. Thermodynamic factors that influence the ATZ adsorption by a MgO/activated carbon nanocomposite at various temperatures.

T (K)	ΔG (J/mol)	ΔH (kJ/mol)	ΔS (J mol/K)
308	-5487.26	55.67	198.87
313	-6731.3		
318	-7518.72		
323	-8534.42		

(a)

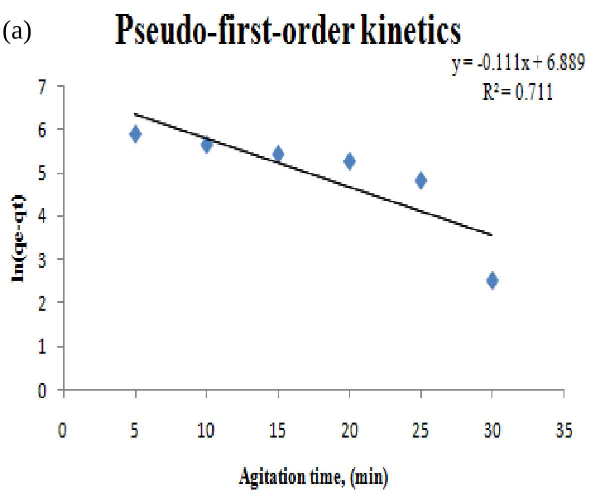

(b)

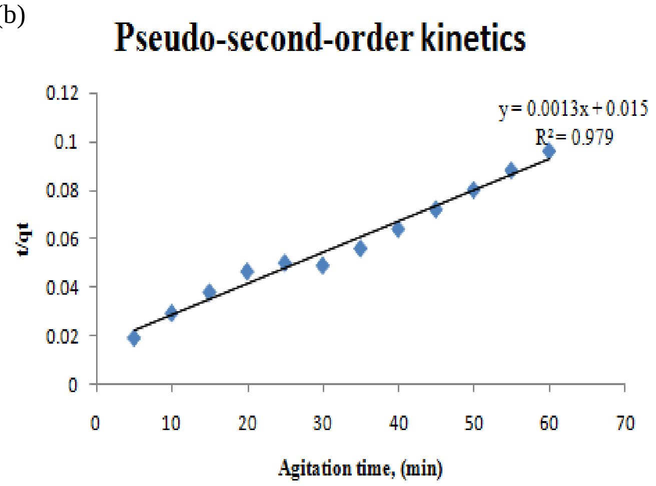

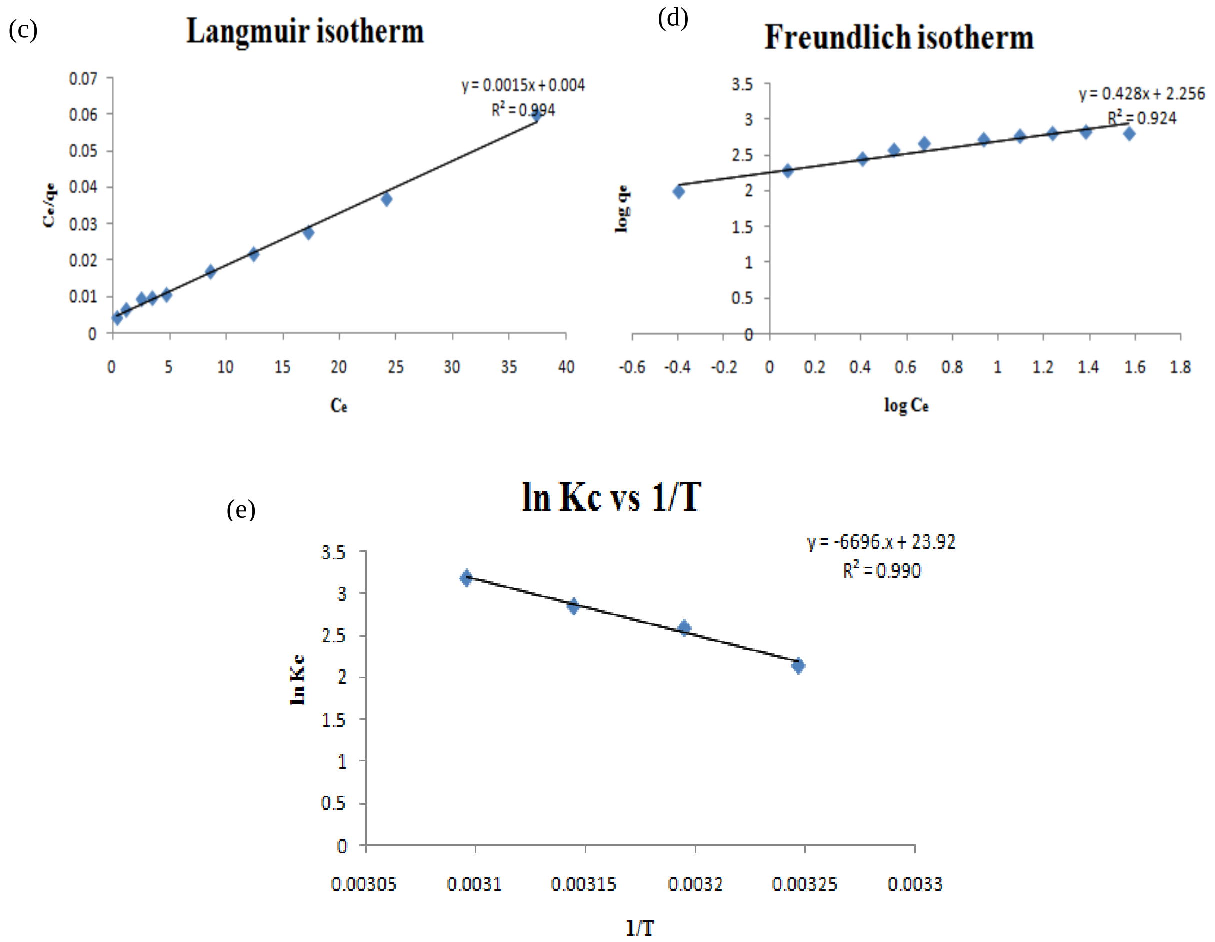

Figure.4. (a) Pseudo-first-order kinetics, (b) Pseudo-second-order kinetics, (c) Langmuir isotherm model, (d) Freundlich isotherm model, (e) Thermodynamics

Figures 4 (c) and 4 (d) display the fitting graphs for these models (d). The Langmuir model can more accurately represent the adsorption data because to its higher R2 value (0.994) compared to the Freundlich model's (0.924). ATZ has an adsorption capability of 666.6 mg/g. This number is in good agreement with the experiment's measured adsorption capacity [16, 17].

The thermodynamic parameters can be calculated using the data from Fig. 4 (e) and are shown in Table 1. It appears to show that the adsorption process was both impulsive and thermodynamically feasible because ΔG was negative at different temperatures. The minor temperature rise in the ΔG values suggests that at higher temperatures, more ATZ was adsorbed onto the adsorbent surface. ATZ adsorption is therefore supported at higher temperatures. Positive ΔH and ΔS values suggest endothermia, as well as an increase in unpredictability at the phase borders throughout the adsorption process.

4. Conclusions

Magnesium oxide nanoparticles were produced using precipitation, and a MgO/activated carbon nanocomposite was subsequently produced and investigated using SEM, XRD, and FTIR. The MgO/activated carbon production method was used to remove ATZ from the aqueous solution. The system's kinetics, isotherms, and thermodynamics of adsorption for removing ATZ from aqueous solution were examined in batch investigations. Under ideal conditions, the MgO/activated carbon combination removed 96 percent of the ATZ, outperforming the vast majority of other adsorbents for ATZ removal found in the literature. The maximal adsorption capacity was determined to be 625.5 mg/g. Our findings indicate that MgO/activated carbon could be used as an adsorbent since it has a better capacity for adsorbing ATZ. MgO/activated carbon nanocomposite may have been identified as the most effective and advantageous technique for ATZ adsorption as a result.

References

1. Ali, I., ALOthman, Z.A. & Al-Warthan, A. Sorption, kinetics and thermodynamics studies of ATZ herbicide removal from water using iron nano-composite material. Int. J. Environ. Sci. Technol. 13, (2016) 733–742.

2. X.M. Yan, B.Y. Shi, J.J. Lu, C.H. Feng, D.S. Wang, H.X. Tang, Adsorption and desorption of ATZ on carbon nanotubes, Journal of Colloid and Interface Science, 321(1), (2008), 30-38.
3. Heena Khawaja, Erum Zahir, Muhammad Asif Asghar, Kashif Rafique & Muhammad Arif Asghar, Synthesis and Application of Covalently Grafted Magnetic Graphene Oxide Carboxymethyl Cellulose Nanocomposite for the Removal of ATZ From an Aqueous Phase, Journal of Macromolecular Science, Part B, 60:12, (2021) 1025-1044.
4. Bandela Sowjanya, U. Sirisha, Alpitha Suhasini Juttuka, Sreenivas Matla, Pulipati King, Meena Vangalapati, Synthesis and characterization of zinc oxide nanoparticles: It's application for the removal of alizarin red S dye, Materials Today: Proceedings, 62(6), (2022) 3968-3972.
5. Mata Subhashita, Thanusha Punugoti, Bandela Sowjanya, Venkat Rao Poiba & Meena Vangalapati, Synthesis of Cu/ZnO nanoparticles and its exploitation as a catalyst for the removal of Cetrimonium Bromide, Advances in Materials and Processing Technologies (2021).
6. R.T. De Silva, M.M.M.G.P.G. Mantilaka, S.P. Ratnayake, G.A.J. Amaratunga, K.M. Nalin de Silva, Nano-MgO reinforced chitosan nanocomposites for high performance packaging applications with improved mechanical, thermal and barrier properties, Carbohydrate Polymers, 157, (2017), 739-747.
7. Mohammad Shirmardi, Nadali Alavi, Eder C. Lima, Afshin Takdastan, Amir Hossein Mahvi, Ali Akbar Babaei, Removal of ATZ as an organic micro-pollutant from aqueous solutions: a comparative study, Process Safety and Environmental Protection,103(A), (2016), 23-35.
8. Murilo B. Andrade, Tássia R. T. Santos, Marcela Fernandes Silva, Marcelo F. Vieira, Rosângela Bergamasco & Safia Hamoudi, Graphene oxide impregnated with iron oxide nanoparticles for the removal of ATZ from the aqueous medium, Separation Science and Technology, 54(16), (2019) 2653-2670.
9. Elsharkawy, Rehab. Framework of nano metal oxides N-NiO@ N-Fe3O4@ N-ZnO for Adsorptive removal of atrazine and Bisphenol-A from Wastewater: Kinetic and Adsorption studies. Environmental Nanotechnology, Monitoring & Management, (2021).
10. V.R. Myneni, Thanusha punugoti, N. Sasi Kala, N.R. Kanidarapu, Meena Vangalapati, Modelling and Optimization of Methylene Blue Adsorption onto Magnesium Oxide Nanoparticles loaded onto Activated Carbon (MgO/activated carbon): Response Surface Methodology and Artificial Neural Networks, Materials Today: Proceedings, 18(7), (2019) 4932-4941.
11. Gowthami V, Sowjanya B, Kumar MN, Vangalapati M. 2023. Synthesized MgO/Chitosan Nanocomposite: It's Application for the Removal of Dicofol and Optimization by Box Benhken Design. *Nano World J* 9(1): 1-7.
12. Kuchi Chandrika, Ashwarya Chaudhary, Tejaswi Mareedu, U. Sirisha, Meena Vangalapati, Adsorptive removal of acridine orange dye by green tea/copper-activated carbon nanoparticles (Gt/Cu-AC np), Materials Today: Proceedings, 44(1), (2021), 2283-2289.
13. Fan Zhang, Xin Chen, Fenghuang Wu, Yuefei Ji, High adsorption capability and selectivity of ZnO nanoparticles for dye removal, Colloids and Surfaces A: Physicochemical and Engineering Aspects, 509, (2016), 474-483.
14. U. Sirisha, Bandela Sowjanya, H. Rehana Anjum, Thanusha Punugoti, Ahmed Mohamed, Meena Vangalapati, Synthesized TiO2 nanoparticles for the application of photocatalytic degradation of synthetic toxic dye acridine orange, Materials Today: Proceedings, Volume 62, Part 6, 2022, Pages 3444-3449.
15. N. Sasikala Reddy, N. Lokeswara Reddy, S. Monica Nissy, G. Pallavi, Meena Vangalapati, Degradation of dicofol by synthesized ZnO nanoparticles as catalyst, Materials Today: Proceedings,Volume 26, Part 2, 2020, Pages 1694-1700.
16. Shaviz Soudagar, Sahukaru Akash, Marupudi Sree Venkat, Venkata Rao Poiba, Meena Vangalapati, Adsorption of methylene blue dye on nano graphene oxide-thermodynamics and kinetic studies, Materials Today: Proceedings, Volume 59, Part 1, 2022, Pages 667-672.
17. Singarapu Sai Santosh, K. Mani Divya, N. Sasikala, D.V. Surya Prakash, Meena Vangalapati, Enhanced catalyst performance copper doped ZnO nanoparticles for removal of dicofol, Materials Today: Proceedings, Volume 26, Part 2, 2020, Pages 1718-1722.